THE FASEB JOURNAL • RESEARCH • www.fasebj.org

Activating β-catenin/Pax6 axis negatively regulates osteoclastogenesis by selectively inhibiting phosphorylation of p38/MAPK

Zhiwei Jie,[*,†,1] Shuying Shen,[*,†,1] Xiangde Zhao,[*,†,1] Wenbin Xu,[*,†] Xuyang Zhang,[*,†] Bao Huang,[*,†] Pan Tang,[‡] An Qin,[§] Shunwu Fan,[*,†,2] and Ziang Xie[*,†,3]

[*]Department of Orthopaedic Surgery, Sir Run Run Shaw Hospital, Zhejiang University School of Medicine, Hangzhou, China; [†]Key Laboratory of Musculoskeletal System Degeneration and Regeneration Translational Research of Zhejiang Province, Hangzhou, China; [‡]Department of Orthopaedics, Huzhou Hospital, Zhejiang University, Hangzhou, China; and [§]Department of Orthopaedics, Shanghai Key Laboratory of Orthopaedic Implant, Shanghai Ninth People's Hospital, Shanghai Jiao Tong University School of Medicine, Shanghai, China

ABSTRACT: Balance of osteoclast formation is regulated by the receptor activator of NF-κB ligand and extracellular negative regulators such as IFN-γ and IFN-β. However, very little is known about the intrinsic negative regulatory factors of osteoclast differentiation. Recently, the paired-box homeodomain transcription factor Pax6 was shown to negatively regulate receptor activator of NF-κB ligand–mediated osteoclast differentiation. However, the mechanism underlying this regulation is still unclear. In this study, we show that a p38 inhibitor (VX-745) up-regulates the expression of Pax6 during osteoclast differentiation. Subsequently, we found that β-catenin could bind to the proximal region of *Pax6* promoter to induce its expression, and this action could be impaired by p38-induced ubiquitin-mediated degradation of β-catenin. Our results suggest that *Pax6* is regulated by a novel p38/β-catenin pathway. Pax6 can further regulate the nuclear translocation of NF of activated T cells, cytoplasmic 1. Our study indicates that this novel p38/β-catenin/Pax6 axis contributes to negative regulation of osteoclastogenesis. In addition, our study proposes a novel approach to treat osteoclast-related diseases through the use of VX-745 complemented with the β-catenin activator SKL2001.—Jie, Z., Shen, S., Zhao, X., Xu, W., Zhang, X., Huang, B., Tang, P., Qin, A., Fan, S., Xie, Z. Activating β-catenin/Pax6 axis negatively regulates osteoclastogenesis by selectively inhibiting phosphorylation of p38/MAPK. FASEB J. 33, 000–000 (2019). www.fasebj.org

KEY WORDS: bone loss · osteoclast · VX-745 · SKL2001 · therapeutic

Bone homeostasis is controlled by a fine balance between bone resorption and bone formation (1). Osteoclast (OC) is regarded as the only type of cell with the ability to degrade bone through the process of bone resorption (2). OC precursors (pre-OCs) expressing receptor activator of NF-κB (RANK) and receptor of M-CSF (c-Fms) can differentiate into functional multinucleated cells in the presence of 2 critical factors, receptor activator of NF-κB ligand (RANKL) and M-CSF (3). In fact, M-CSF promotes the proliferation and survival of bone marrow–derived macrophages (BMMs) by binding to the receptor c-Fms (4). Conversely, RANKL binds to the receptor of RANK, subsequently triggers the induction of OC-specific genes, including NF of activated T cells, cytoplasmic 1 (NFATc1), dendritic cell–specific transmembrane protein, cathepsin K (CTSK), and tartrate-resistant acid phosphatase (TRAP) (5, 6). The expression of these genes is regulated by transcription factors such as PU.1, AP-1, and NF-κB, which act as downstream signaling events to RANKL–RANK signaling (7, 8). The MAPK cascade is another vital signaling pathway involved in osteoclastogenesis (9). Except for the ERK and JNK MAPK family, p38 MAPK has long been closely related to cell differentiation and inflammatory responses (10). In particular, it has been shown that p38 MAPK regulates OC-specific genes during OC differentiation (11). However, the presence of other mechanisms for p38-mediated regulation of osteoclastogenesis has not been investigated.

ABBREVIATIONS: BMM, bone marrow–derived macrophage; BV, bone volume; ChIP, chromatin immunoprecipitation; CTSK, cathepsin K; NFATc1, NF of activated T cells, cytoplasmic 1; OC, osteoclast; OC.S/BS, osteoclast surface area per bone surface area; RANKL, receptor activator of NF-κB ligand; siRNA, small interfering RNA; TRAP, tartrate-resistant acid phosphatase

[1] These authors contributed equally to this work.
[2] Correspondence: Department of Orthopaedics, Sir Run Run Shaw Hospital, Zhejiang University School of Medicine, 3rd Qingchun Rd., Hangzhou, China. E-mail: shunwu_fan@zju.edu.cn
[3] Correspondence: Department of Orthopaedics, Sir Run Run Shaw Hospital, Zhejiang University School of Medicine, 3rd Qingchun Rd., Hangzhou, China. E-mail: ziang_xie@zju.edu.cn

doi: 10.1096/fj.201801977R
This article includes supplemental data. Please visit *http://www.fasebj.org* to obtain this information.

Paired-box (Pax) homeodomain genes encode numerous transcription factors that are key regulators of growth in a wide range of tissues and organs across rich and varied species (12, 13). Among them, Pax5 reportedly acts as both a transcriptional activator and a transcriptional repressor in mice lacking Pax5 with severe osteopenia. However, Pax5 was not detected in osteoblasts or in OCs (14). In contrast, Hinoi *et al.* (15) found that Pax5 promotes osteoblastogenesis through direct induction of osteorix and osteocalcin. Thus, conclusions can be made regarding the regulation of bone homeostasis by the Pax gene. Interestingly, another key gene of the Pax gene family, Pax6, is reportedly a negative regulator in RANKL-induced osteoclastogenesis. Pax6 can attenuate primary OC differentiation and promoter activity of the NFATc1-mediated activation of Acp5 gene (16). This regulation of osteoclastogenesis is similar to RANKL-induced activation of the IFN-β or IFN-γ gene, which constitutes a critical aspect of the negative feedback regulation of RANKL signaling for preventing excessive bone resorption (17). It has been shown that Pax6 can respond to MAPK-mediated signals in all the tissues where it is expressed during development (18). Furthermore, Hadjal *et al.* (19) reported that p38 regulates Pax6 expression *via* the p53 cascade in embryonic stem cells. It has therefore been suggested that Pax6 might be regulated by the MAPK signaling pathway in several cells.

However, the role of RANKL–RANK signaling in the induction of Pax6 is not yet understood. The goal of the present study was to elucidate possible novel mechanisms to explain the Pax6-induced negative regulation of osteoclastogenesis. Moreover, we explored the novel possibility of using a p38 selective inhibitor, VX-745 (20), and a β-catenin agonist, SKL2001, as treatment for osteolytic diseases.

MATERIALS AND METHODS

Reagents

VX-745 and SKL2001 were purchased from Selleck (Shanghai, China), DMSO was purchased from MilliporeSigma (Burlington, MA, USA), and Cell Counting Kit-8 was obtained from Dojindo Molecular Technology (Kumamoto, Japan). Recombinant soluble mouse M-CSF and mouse RANKL were obtained from R&D Systems (Minneapolis, MN, USA). VX-745 was dissolved in DMSO and stored at −20°C. Specific antibodies p38α, p-p38 (Thr180/Tyr182), c-Fos, NFATc1, β-catenin, p-β-catenin (S33), TRAP, Pax6, and β-actin were obtained from Abcam (Shanghai, China). The TRAP staining kit and all other reagents were purchased from MilliporeSigma, unless otherwise stated.

BMM preparation and OC differentiation

Primary BMMs were isolated from the whole bone marrow of male 6-wk-old C57BL/6 mice as previously described (21). Cells were isolated from the femoral and tibial bone marrow and cultured in α-MEM supplemented with 10% FBS, 1% penicillin/streptomycin, and 25 ng/ml M-CSF in an incubator with 5% CO_2 at 37°C until they reached 90% confluence. The BMMs were seeded into 96-well plates at a density of 8×10^3 cells/well, in triplicate, in the presence of 25 ng/ml M-CSF, 50 ng/ml RANKL, and different concentrations of VX-745 or SKL2001 or small interfering RNA (siRNA). Untreated cells were included as controls. The culture medium was replaced every 2 d, and OCs were cultured for 7 d. Afterward, the cells were washed twice with PBS, fixed in 4% paraformaldehyde for 30 min, and stained with TRAP. TRAP-positive cells with >5 nuclei were considered OCs.

Bone resorption assay

BMMs were seeded at a density of 2×10^4 cells/well in the presence of 25 ng/ml M-CSF and 50 ng/ml RANKL. After 4 d, the cells were seeded onto bovine bone slices, in triplicate, at 50 nM VX-745 concentrations, and maintained for an additional 3 d. Untreated cells were used as a control. Resorption pits were imaged by using a scanning electron microscope (FEI Quanta 250; Thermo Fisher Scientific, Waltham, MA, USA), and the bone resorption area was quantified by using ImageJ software (National Institutes of Health, Bethesda, MD, USA).

RNA extraction and quantitative PCR

RNA extraction and quantitative PCR assay were performed according to a previous study (21). Specificity of amplification was verified by performing RT-PCR and analyzing the melting curves. Mouse *Gapdh*, *Ctsk*, *Trap*, *c-Fos*, *Nfatc1*, *Pax1*, *Pax2*, *Pax3*, *Pax4*, *Pax5*, *Pax6*, *Pax7*, *Pax8*, and *Pax9* primer sequences are presented in Supplemental Table S1.

Chromatin immunoprecipitation assays

Cell extraction was prepared by using the Chromatin Immunoprecipitation Kit (9002; Cell Signaling Technology, Danvers, MA, USA) according to the manufacturer's protocol. In brief, pre-OCs were treated with or without SKL2001 in the stimulation with 50 ng/ml RANKL for 24 h; pre-OCs were treated with 1% formaldehyde for 10 min to crosslink chromatin and protein, collected, and digested to produce chromatin fragments for incubation with IgG or specific antibodies for β-catenin, respectively. The immunoprecipitates were then incubated with protein A/G agarose beads. After several washes, the protein-DNA complex was reversed. At the end, DNA from the chromatin immunoprecipitation (ChIP) assays was amplified and analyzed by using PCR. Primer sequences are presented in Supplemental Table S2.

In vitro gene knockdown experiments

BMMs were transfected with 10 nM siRNA using Lipofectamine 3000 (Thermo Fisher Scientific) for 4 h. After the medium was changed, cells were incubated overnight before RANKL treatment. The sequences of siRNA are shown in Supplemental Table S3.

Western blot assay

Cells were incubated in RIPA buffer (Cell Signaling Technology) supplemented with 100 mM PMSF and phosphatase inhibitor (Cell Signaling Technology) on ice, followed by centrifugation at 12,000 rpm for 15 min to isolate the supernatant. Proteins were resolved by 10% SDS-PAGE and transferred to PVDF membranes (Bio-Rad, Hercules, CA, USA) by electroblotting. The membranes were blocked with 5% nonfat dry milk in TBST at room temperature for 1 h and then incubated with primary

antibodies overnight at 4°C. Protein bands were developed by using a horseradish peroxidase–conjugated goat–anti-rabbit or goat–anti-mouse IgG (Abcam), followed by detection with ECL reagent (MilliporeSigma). Protein bands were visualized by using the LAS-4000 Science Imaging System (Fujifilm, Tokyo, Japan), and the obtained images were analyzed with ImageJ software.

Coimmunoprecipitation assay

Briefly, cell extracts were first precleared with 25 μl of protein A/G-agarose (50% v/v). The supernatants were immunoprecipitated with 2 μg of anti-Pax6 and anti–β-catenin antibodies overnight at 4°C, followed by incubation with protein A/G-agarose 4 h at 4°C. Protein A/G-agarose-antigen-antibody complexes were collected by centrifugation at 12,000 rpm for 60 s at 4°C. The pellets were washed 5 times with 1 ml of IPH buffer (50 mM Tris-HCl, pH 8.0, 150 mM NaCl, 5 mM EDTA, 0.5% Nonidet P-40, and 0.1 mM PMSF) for 5 min each time at 4°C. Bound proteins were resolved by SDS-PAGE, followed by Western blotting with anti-NFATc1 and anti-ubiquitin antibodies. The experiments were replicated ≥3 times.

Immunofluorescence staining assay

BMMs were seeded at a density of 8×10^3 cells in 96-well plates. After being stimulated with M-CSF and RANKL for 3 d, the cells were treated with siRNA or SKL2001 for 24 or 48 h. After incubation, cells were washed twice with PBS, fixed in 4% paraformaldehyde for 30 min, and then washed with PBS 3 times before permeabilization with 0.1% Triton-X100 for 30 min at room temperature. After blocking with 1% BSA-PBS for 1 h at room temperature, cells were incubated with anti-CTSK antibody and anti–β-catenin antibody diluted 1:200 in 1% BSA-PBS at 4°C overnight. Nuclei were stained with 0.1 μg/ml DAPI (MilliporeSigma) in PBS at room temperature for 10 min in the dark. After being washed 3 times with PBS, the cells was imaged by using a fluorescence microscope (BX51TRF; Olympus, Tokyo, Japan), and the quantification of the image was analyzed by using ImageJ software.

In vivo bone loss experiments

Eight-week-old female C57BL/J6 mice were implanted with collagen sponges soaked with PBS or RANKL (1 μg) in the middle of the calvaria as previously described (22). The compounds were injected onto the calvaria every day, at indicated times. After 6 d, the calvaria were subjected to micro–computed tomography and histologic analyses.

Animal experiments were approved by the Committees on the Care and Use of Animals in Research at Sir Run Run Shaw Hospital. All animals were kept in a specific pathogen-free facility with a 12-h light/dark cycle.

Micro-computed tomography scanning

The fixed calvarial bones were analyzed by using a high-resolution micro–computed tomography (1072; SkyScan, Aartselaar, Belgium) instrument. After reconstruction, a square region of interest, set at 0.5 mm from the calvarial bone, was selected for further qualitative and quantitative analyses. Trabecular bone volume (BV) per total volume was determined for each sample, as previously reported (23).

Bone histomorphometry

Histomorphometry analysis was performed as previously reported (24). Fixed calvarial bones were decalcified in 10% EDTA for 2 wk and embedded in paraffin. Histologic sections were prepared for TRAP and immunofluorescence staining. The ratio of OC surface area per bone surface area (OC.S/BS) was assessed in each sample. The Pax6-positive cell area normalized to the BS was analyzed in each sample. The quantification of the image was analyzed by using ImageJ software.

Statistical analysis

Results are expressed as means ± SD. Statistical analyses were performed by using Prism 6 (GraphPad Software, La Jolla, CA, USA). Statistical differences were assessed by using a Student's *t* test or 1-way ANOVA followed by Tukey's *post hoc* analysis where appropriate. Values of $P < 0.05$ were considered statistically significant.

RESULTS

Pax6 expression is up-regulated by p38 inhibitor VX-745 during osteoclastogenesis

Cell viability assay was performed to analyze the potential cytotoxicity of VX-745, a p38 inhibitor, against BMMs (Supplemental Fig. S1*A*). A concentration of 20 nM of VX-745 did not affect the cell viability of BMMs. Furthermore, we found that VX-745 exhibited a better inhibitory effect on OC formation and bone resorption at a lower concentration compared with the classic p38 inhibitor SB20385 (50 nM) (**Fig. 1*A*, *B***). Interestingly, we also found that the expression of *Pax6* mRNA was up-regulated during OC differentiation (Fig. 1*C*). Furthermore, BMMs treated with VX-745 (50 nM) in the presence of M-CSF and RANKL for 5 d unexpectedly showed that the mRNA and protein levels of Pax6 were increased even under these conditions (Fig. 1*D–F*). In addition, quantitative PCR analysis revealed that treatment with VX-745 could accelerate the expression of *Pax6* during different periods of osteoclastogenesis in BMMs (Fig. 1*E*). Together, these results indicate that treatment with the p38 inhibitor VX-745 induces the expression of *Pax6* and negatively regulates OC differentiation.

Silencing of Pax6 reversed the suppression of osteoclastogenesis by promoting the nuclear translocation of NFATc1 at a late stage of OC formation

To investigate the role of Pax6 in OC differentiation, we knocked down the expression of *Pax6* at a late stage (on d 4) during OC differentiation. Silencing of *Pax6* reversed the suppression of OC formation and bone resorption (**Fig. 2*A*, *B***). This finding suggests that Pax6 negatively regulated the OC formation largely during the late stage of OC differentiation. To further confirm this theory, Western blot assay was performed, and we found that the expression of NFATc1 was not altered upon silencing of *Pax6*. However, the mRNA and protein expression levels of

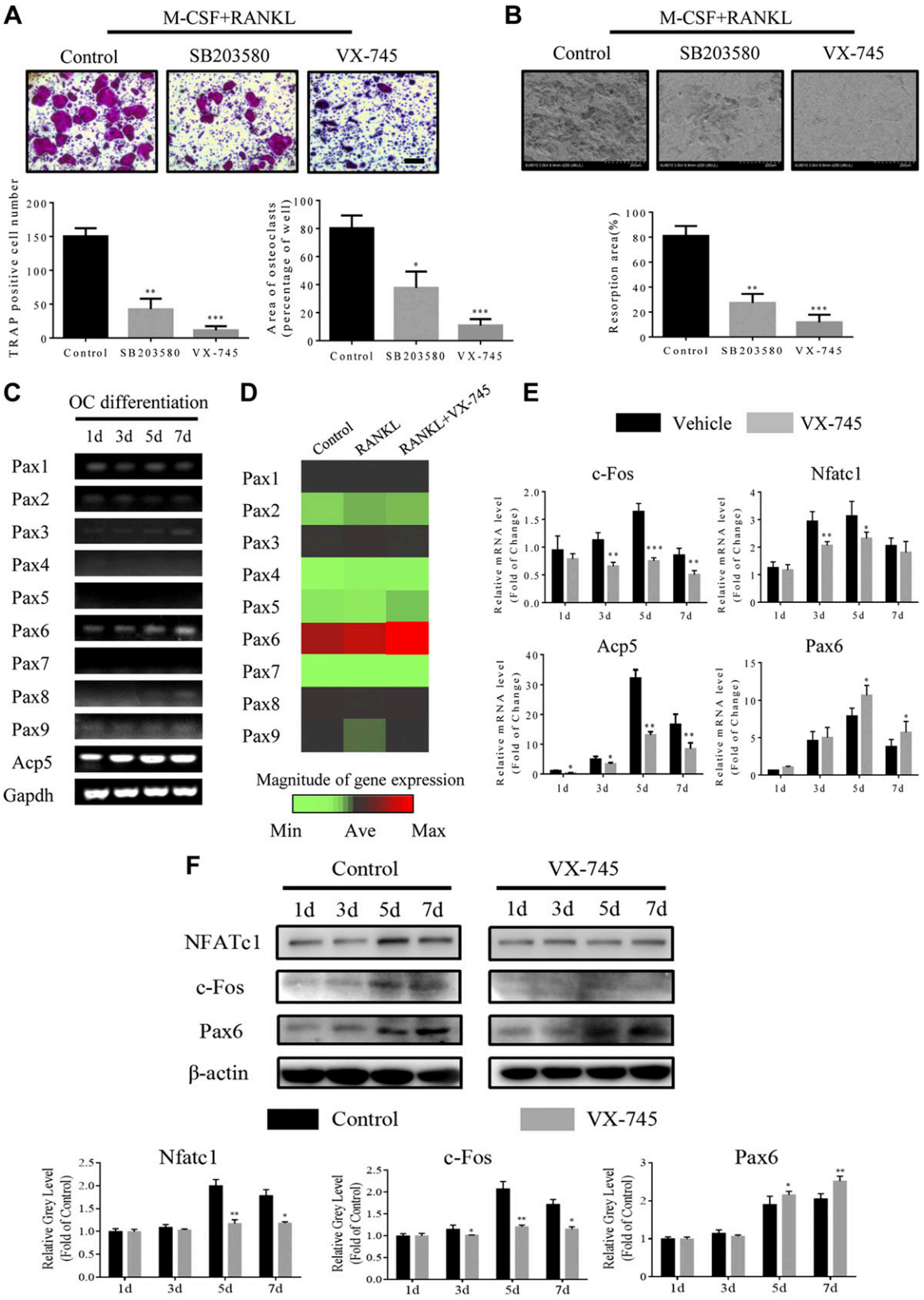

Figure 1. Up-regulated expression of Pax6 after treatment with VX-745. *A*) TRAP staining of BMMs cultured with M-CSF and RANKL for 7 d in the presence of SB203580 (50 nM) or VX-745 (50 nM). *B*) Bone slice assay indicated the effects of compounds on bone resorption. *C*) Real-time PCR analysis of expression of Pax family genes during OC differentiation. *D*) Heatmap of gene expression of Pax families posttreatment with VX-745 for 5 d. *E*, *F*) Quantitative real-time PCR and Western blot analysis of Pax6 and OC-related gene expression during OC differentiation in the absence or presence of VX-745. All experiments were performed ≥3 times; data are presented as means ± SD. Scale bar, 100 μm. Student's *t* test analysis was performed. $*P < 0.05$, $**P < 0.01$, $***P < 0.005$, compared with the control group.

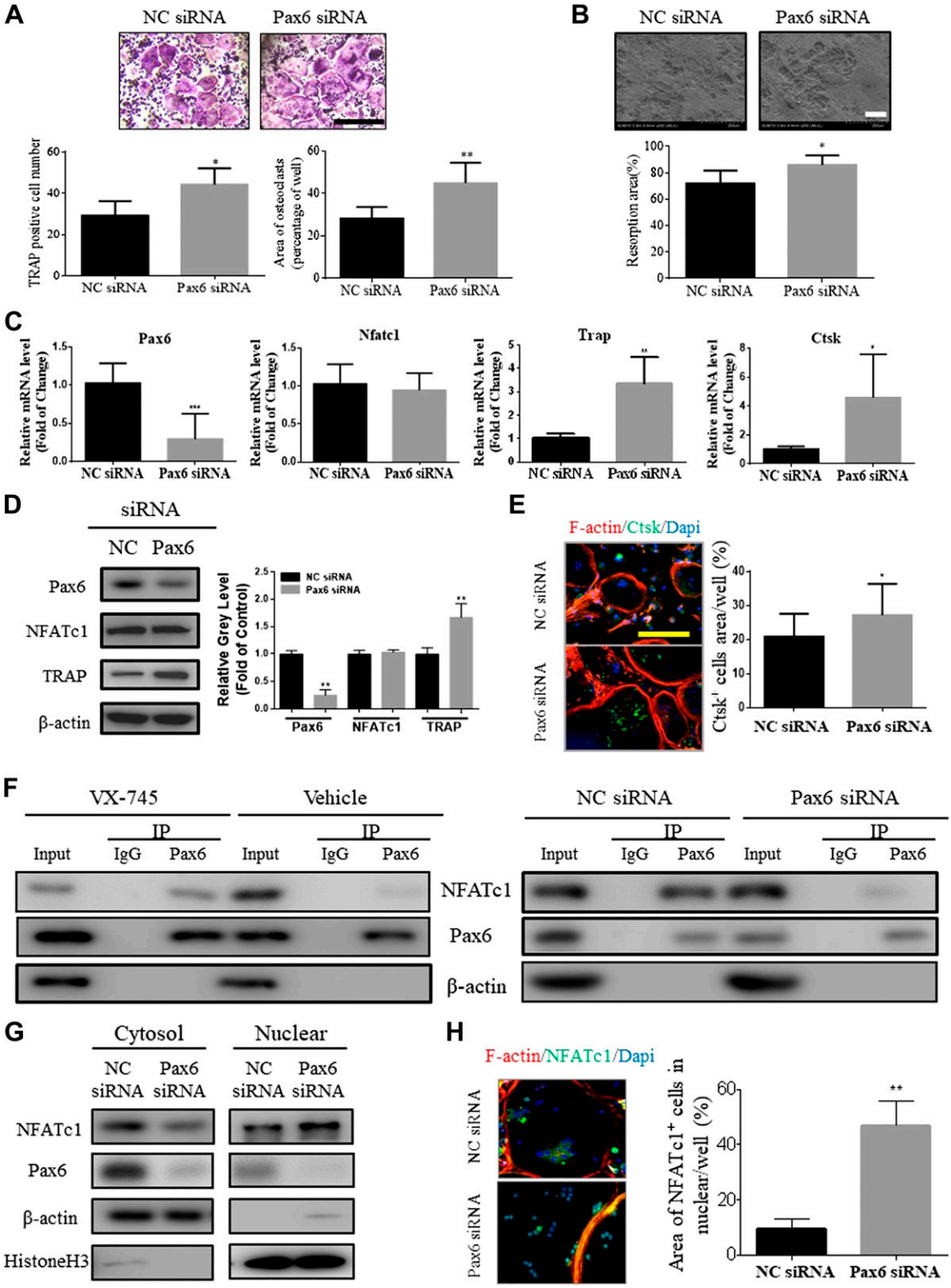

Figure 2. Pax6 regulates osteoclastogenesis by suppressing the expression of TRAP through its interaction with NFATc1. *A*) TRAP staining assay on pre-OCs transfected with negative control (NC) siRNA or Pax6-targeted siRNA on d 4 during OC differentiation (M-CSF 25 ng/ml, RANKL 12.5 ng/ml). *B*) Transfected pre-OCs cultured with M-CSF and RANKL on bone slice. Bone resorption areas were analyzed by using ImageJ software. *C*, *D*) Pre-OCs transfected with siRNA on d 4 during OC differentiation, real-time PCR (*C*), and Western blot (*D*), performed to analyze expression of Pax6, Nfatc1, and Trap. *E*) Immunofluorescence assay showing the expression of CTSK. *F*) Immunoprecipitation with Pax6 antibody in transfected pre-OCs (incubated with VX-745 or treated with Pax6 siRNA). The obtained immunoprecipitates were analyzed by using the indicated antibodies. *G*) The expression of different proteins isolated from the cytosol and nuclei samples obtained from pre-OCs analyzed by Western blot. *H*) Immunofluorescence assay showing the nuclear translocation of NFATc1 after treatment with Pax6 siRNA. All experiments were performed ≥3 times; data are presented as means ± SD. Scale bars, 100 μm. Student's *t* test analysis was performed. $^{*}P < 0.05$, $^{**}P < 0.01$, $^{***}P < 0.005$, compared with the control group.

TRAP and CTSK were increased after silencing of *Pax6* (Fig. 2*C, D*). In addition, immunofluorescence assay revealed that the area of CTSK-positive cells in the *Pax6*-siRNA group was more than in the negative control siRNA group (Fig. 2*E*). Given that NFATc1 expression was not altered but protein levels of TRAP and CTSK increased, we next evaluated whether silencing of *Pax6* affected the nuclear translocation of NFATc1 to alter the transcription of *Trap* and *Ctsk*. Co-immunoprecipitation assay showed that silencing of *Pax6* reduced the interaction between Pax6 and NFATc1, which promotes the nuclear translocation of NFATc1 to induce the expression of OC-related genes such as *Trap* and *Ctsk* (Fig. 2*C, F–H*). In addition, treatment with VX-745 partially inhibited the nuclear translocation of NFATc1 by enhancing the interaction between Pax6 and NFATc1 (Fig. 2*F*). Collectively, these results indicate that *Pax6* suppresses OC formation by reducing the nuclear translocation of NFATc1.

Late stage of OC formation is inhibited by β-catenin–induced expression of *Pax6*

Previous studies have shown that β-catenin induction is required for M-CSF–mediated precursor proliferation, and its degradation is required for RANKL-mediated OC differentiation (25). Moreover, β-catenin could regulate Pax6 in stem cells (26). Therefore, we next investigated whether this balance between induction and degradation of β-catenin at a late stage of OC formation could affect Pax6 during OC differentiation. First, we knocked down the expression of β-catenin using siRNA at a late stage (treated on d 4) during OC differentiation. Silencing of β-catenin at the late stage promoted OC formation and bone resorption (**Fig. 3*A, B***). Consistent with the results of the TRAP staining assay, silencing of β-catenin at a late stage during OC formation could reduce the expression of Pax6 but induce the expression of TRAP without affecting NFATc1 levels (Fig. 3*C*). Subsequently, we treated BMMs with SKL2001 (cell viability assay shown in Supplemental Fig. S1*B*), a β-catenin activator, at the early (on d 2) or late stage time points during OC differentiation. Interestingly, we found that the proliferation of BMMs was promoted and the number of OCs was increased with a smaller size by treatment with Wnt3a or SKL2001 (20 μM) at an early stage, although the area occupied by OCs was not altered (Fig. 3*D*). However, both the number and the area of OCs were inhibited by treatment with Wnt3a or SKL2001 at the late stage (Fig. 3*E*). Moreover, Western blot and immunofluorescence assays verified that SKL2001 promoted the nuclear translocation of β-catenin in pre-OCs in the presence of M-CSF and RANKL (Fig. 3*F, G*). In agreement with this, SKL2001 induced the expression of Pax6 to decrease the expression of TRAP (Fig. 3*H*). More importantly, ChIP assay confirmed that β-catenin can bind to the promoter region of *Pax6* in pre-OCs, and SKL2001 promoted this binding (Fig. 3*I*). Thus, β-catenin can induce Pax6 expression to inhibit OC formation during the late stages of osteoclastogenesis.

Pax6 may negatively regulate osteoclastogenesis *via* reduced p38-induced ubiquitin-mediated degradation of β-catenin at a late stage of OC formation

We next investigated possible mechanisms underlying the RANKL–RANK signaling– induced Pax6 at a late stage of osteoclastogenesis. Intriguingly, Western blot analysis showed that RANKL enhanced the phosphorylation of β-catenin at S33, whereas treatment with VX-745 reduced the phosphorylation of p38 as well as of β-catenin at S33 at a late stage (d 4) of OC formation (**Fig. 4*A***). Furthermore, treatment of BMMs with the proteasome inhibitor MG132 indicated that VX-745 inhibited the ubiquitination of β-catenin (Fig. 4*B*). In addition, the degradation of β-catenin was blocked when treated with VX-745 in the presence of cycloheximide (Fig. 4*C*). Thus, phosphorylation of β-catenin may mark it for ubiquitin-mediated degradation, and this process seems to be inhibited by treatment with VX-745. In addition, the pre-OCs were treated with negative control siRNA or β-catenin siRNA in the presence or absence of VX-745 at the late stage of OC differentiation. TRAP staining assay revealed that silencing of β-catenin showed increased TRAP expression and OC differentiation, and this action was partially reversed upon VX-745 application (Fig. 4*D*). Moreover, the protein levels showed that the expression of Pax6 treated by silencing of β-catenin was reversed by VX-745 application (Fig. 4*E*). However, when we treated pre-OCs with both SKL2001 and VX-745 at a late stage of OC differentiation, the inhibitory effect on osteoclastogenesis was more effective than that of SKL2001 alone or VX-745 alone (Fig. 4*F*). However, Western blotting assay showed that the expression of Pax6 was dramatically up-regulated by treatment with SKL2001 and VX-745, compared with treatment with SKL2001 alone or VX-745 alone (Fig. 4*G*). Taken together, the results suggest that one possible mechanism for the negative regulation of Pax6 on osteoclastogenesis may be through the inhibition of p38-induced ubiquitin-mediated degradation of β-catenin.

VX-745 synergized with SKL2001 to increase the expression of Pax6 for preventing bone loss *in vivo*

To validate whether VX-745 could act synergistically with SKL2001 to promote the expression of Pax6 for inhibiting osteoclastogenesis *in vivo*, a mouse calvarial bone loss model was used. We first implanted a collagen sponge soaked with RANKL or PBS onto the calvaria where the drug was injected. As expected, there was a significant decrease in BV by RANKL treatment (**Fig. 5*A, D***). Treatment with VX-745 alone slightly increased the BV in the RANKL-implanted group (RANKL/vehicle, 6.22 mm^3; RANKL/VX-745, 9.66 mm^3). Interestingly, treatment with both VX-745 and SKL2001 in the early stage (injection on d 1 after treatment with RANKL) decreased BV compared with VX-745 treatment alone. However, in the late stage (injection on d 4 after treatment with RANKL), treatment with VX-745 and SKL2001 dramatically increased

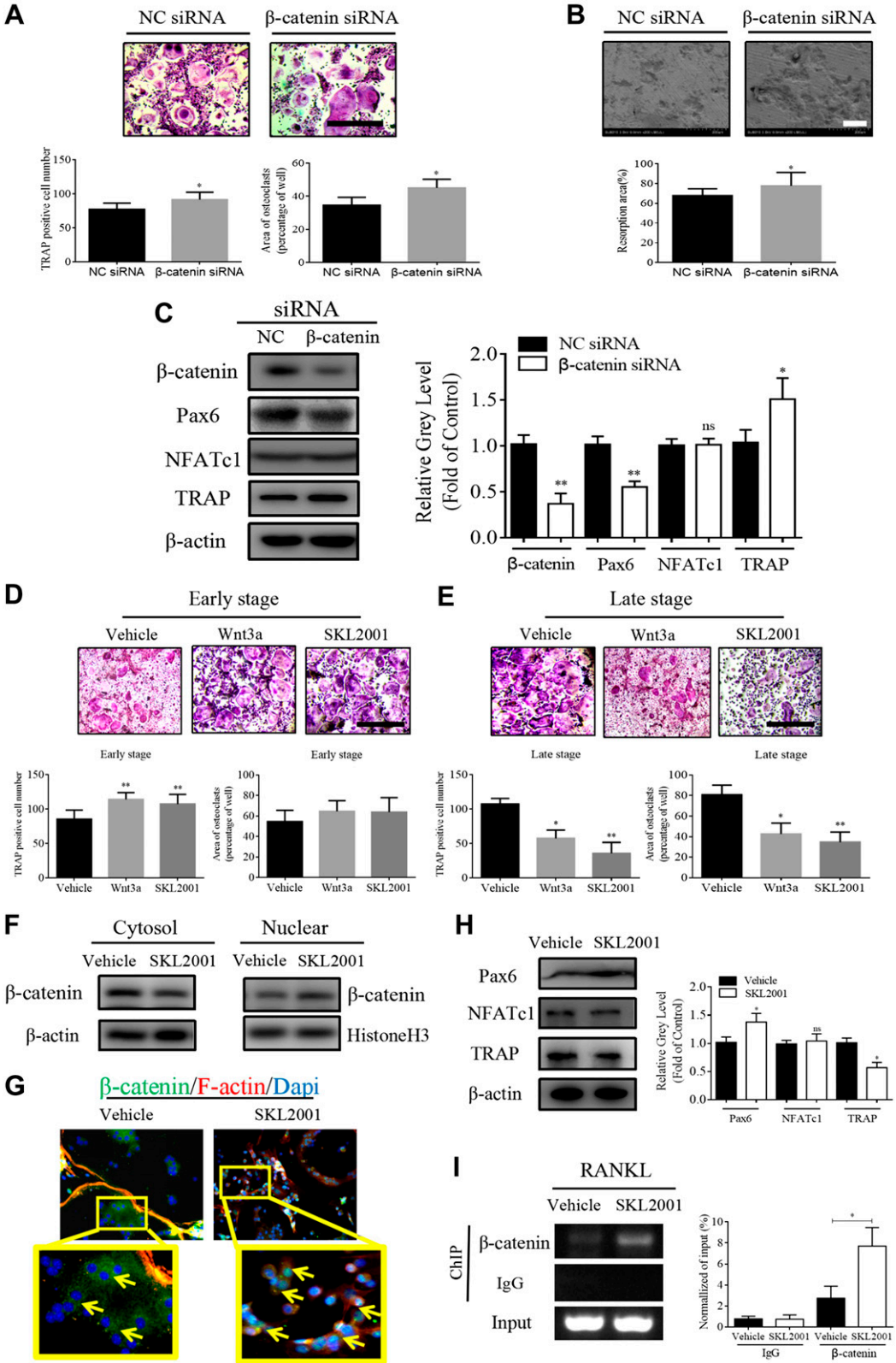

Figure 3. β-catenin mediates the transcription of Pax6 during osteoclastogenesis. *A*) TRAP staining assay on pre-OCs transfected with negative control (NC) or β-catenin–targeted siRNA on d 4 during OC differentiation (M-CSF 25 ng/ml, RANKL 12.5 ng/ml). *B*) Transfected pre-OCs cultured with M-CSF and RANKL on bone slice. Bone resorption areas were analyzed by using ImageJ software. *C*) Western blot performed on pre-OCs transfected with siRNA on d 4 during OC differentiation to analyze expression of β-catenin, Pax6, NFATc1, and TRAP. *D, E*) Pre-OCs were treated with Wnt3a or SKL2001 (20 μM) at an early stage (on d 2) (*D*) or a late stage (on d 4) (*E*) during osteoclastogenesis. *F*) Western blot assay performed to analyze the effect of SKL2001 on nuclear translocation of β-catenin. *G*) Immunofluorescence assay conducted to analyze the effect of SKL2001 on nuclear translocation of

(*continued on next page*)

BV. Thus, treatment with SKL2001 at a late stage had a better efficiency in preventing bone loss *in vivo*. When the calvarial tissue sections were stained with TRAP, the percentage of OC.S/BS was higher in the RANKL-treated group than in the PBS-treated group (Fig. 5*B*). In line with the results of the micro-computed tomography analysis, a significant decrease in OC.S/BS was observed in the VX-745/SKL2001–treated (late stage) group compared with the RANKL-treated group (Fig. 5*B, E*). Furthermore, the immunofluorescence assay showed that the expression of Pax6 was increased upon treatment with both VX-745 and SKL2001 (late stage) (Fig. 5*C, F*). This finding partially indicates that Pax6 is involved in the VX-745–mediated and SKL2001-mediated inhibition of osteoclastogenesis *in vivo*.

DISCUSSION

Multinucleated OCs, formed by the fusion of cells from the monocyte and macrophage family, are regarded as unique cells capable of bone resorption (27). It is well known that excessive OC activity results in bone-related diseases (28). Although several treatments targeting OC exist, more efficient alternatives to the currently available drugs are being investigated (21, 29, 30). Here, we have shown that VX-745, a selective p38 MAPK inhibitor, can inhibit the formation and function of OCs through mechanisms other than the well-known classic pathway. We also showed that VX-745 in combination with SKL2001 (a β-catenin activator) can act as a novel strategy to efficiently prevent bone loss.

Osteoclastogenesis is classically known to be triggered by RANKL–RANK signaling, which activates MAPK and NF-κB–mediated nuclear translocation of c-Fos and NFATc1. It is demonstrated that the p38 MAPK has 4 isoforms: p38α, p38β, p38γ, and p38δ (5, 31, 32). Indeed, a previous study showed that both p38α and p38β knock-out mice exhibited lower bone mass compared with wild-type mice, although this phenotype was mainly affected by osteoblast activity (33). Intriguingly, p38α conditional knockout mice in OCs exhibited distinct alterations in bone resorption at 2.5 and 6 mo of age, and p38α can positively or negatively regulate osteoclastogenesis in different cultural conditions *in vitro* (34). In reality, there are limited studies showing the role of p38 in the selective inhibition on osteoclastogenesis (35, 36). Given these distinct results in OC differentiation, we investigated the additional possible mechanisms involving p38 MAPK signaling during osteoclastogenesis and the effect of p38 inhibition on osteoclastogenesis.

Previous studies have shown that Pax6, a paired-box gene, acts as a transcriptional activator essential for retinal and pancreatic endocrine cell development and the CNS (37). In addition to these roles, we found that Pax6 is induced during osteoclastogenesis and that silencing of *Pax6* promoted OC differentiation by enhancing the nuclear translocation of NFATc1. These results are partially consistent with the previous study (16). Unexpectedly, our data showed that Pax6 was up-regulated after treatment with VX-745 (p38 inhibitor), along with decreased expression of c-Fos and NFATc1. Although many studies report that p38/c-Fos/NFATc1 is the classic pathway promoting OC differentiation (38, 39), we propose that inhibition of p38/Pax6 may act as a negative regulatory pathway for osteoclastogenesis.

To determine the underlying mechanism during osteoclastogenesis regulated by p38/Pax6 pathway, we have predicted the possible transcription factors binding to the promoter of Pax6. To further confirm the prediction, our ChIP assay showed that β-catenin regulated transcription of *Pax6* in the BMMs during the late stage of osteoclastogenesis. Interestingly, silencing of β-catenin by siRNA promoted OC differentiation at a late stage of OC formation, along with decreased expression of *Pax6*. β-catenin is generally regarded as an essential component transducing canonical Wnt signaling during osteoblast differentiation (40). However, Wei *et al.* (25) found that β-catenin could also regulate osteoclastogenesis in a biphasic and dosage-dependent manner. β-catenin induction is required for M-CSF–mediated precursor proliferation, yet its degradation is required for RANKL-mediated OC differentiation. The mechanism underlying this regulation is still unclear. Unexpectedly, in the current study, we found that treatment of BMMs with SKL2001 (a β-catenin activator) in the presence of RANKL promoted osteoclastogenesis at early stages but inhibited osteoclastogenesis during late stages of differentiation. In addition, treatment with SKL2001 at a late stage of OC formation enhanced the expression of Pax6 but reduced the expression of TRAP. These results indicate that Pax6, induced by β-catenin, is involved in OC differentiation.

The p38 MAPKs have been shown to play a role in canonical Wnt/β-catenin signaling, which is important for mineralization and development of osteoprogenitors (33, 41–43). However, the role of p38/β-catenin signaling in osteoclastogenesis is poorly understood. Given that Pax6 was up-regulated by treatment with VX-745, as well as mediated by β-catenin, we investigated the role of p38 signaling in regulating β-catenin during osteoclastogenesis. The results showed that phosphorylation of p38 may promote the phosphorylation of β-catenin at the S33 site, which marks the β-catenin for degradation through ubiquitin-mediated mechanisms (44, 45). In general, in the condition of osteoclastogenesis, degradation of β-catenin may lead to the decreased expression of Pax6. However, we found that Pax6 was up-regulated during osteoclastogenesis, which might be a self-protective mechanism for preventing excessive osteoclastogenesis. Although reduction of β-catenin seems to decrease the expression of Pax6, there

β-catenin. *H*) Western blot assay of pre-OCs, treated or untreated with SKL2001, performed to assess expression of Pax6, NFATc1, and TRAP. *I*) ChIP assay performed on pre-OCs, treated or untreated with SKL2001, in the presence of RANKL. All experiments were performed at ≥3 times; data are presented as means ± SD. Scale bars, 100 μm. Student's *t* test analysis was performed. $^{*}P < 0.05$, $^{**}P < 0.01$, compared with the control group. Ns, not significant.

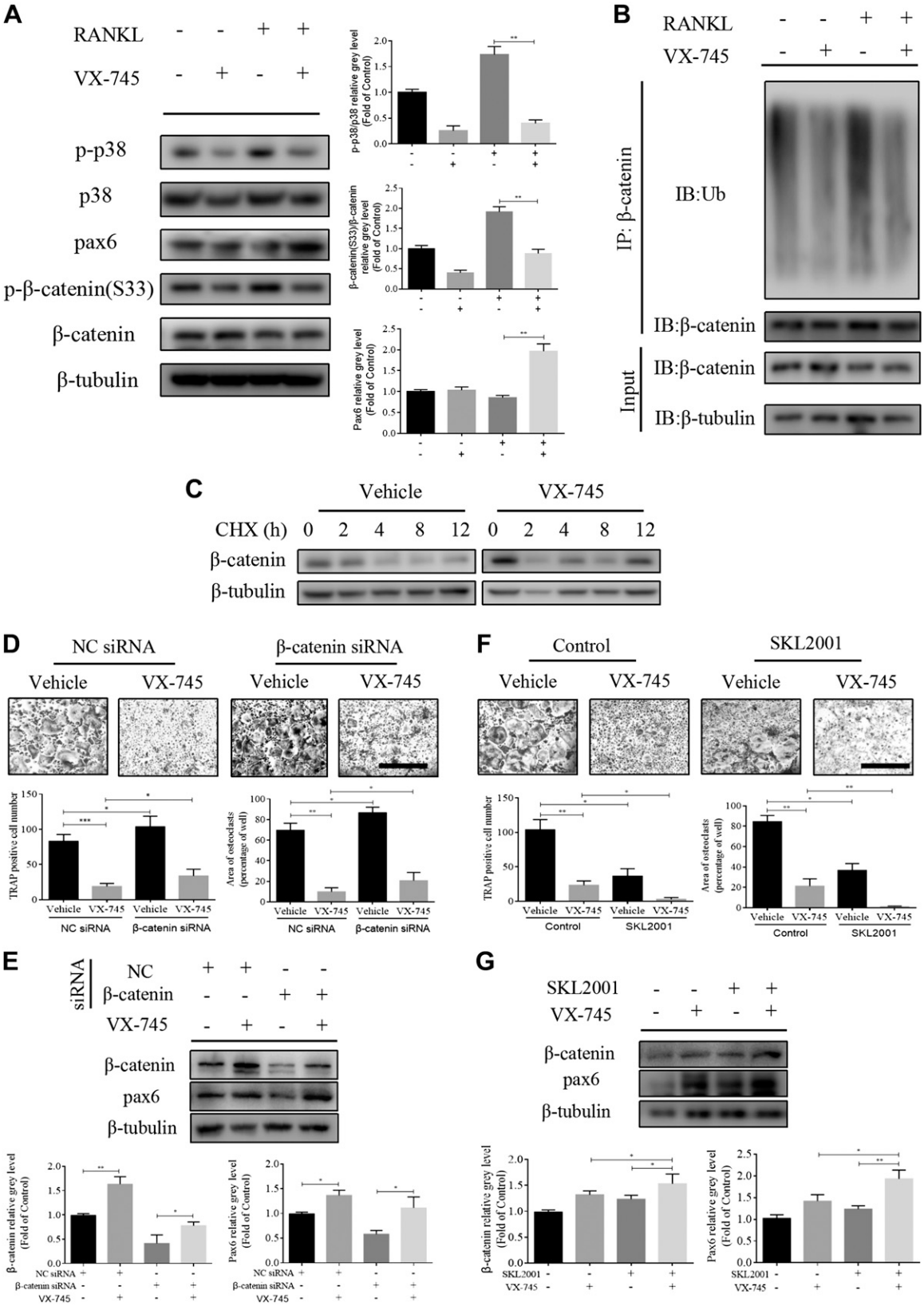

Figure 4. Phosphorylation of p38 mediates the ubiquitination of β-catenin and is involved in the inhibition of osteoclastogenesis by Pax6. *A*) BMMs were treated with VX-745 or RANKL in the presence of M-CSF for 4 d, then for serum starvation, and stimulated with RANKL for 30 min. Indicated proteins were analyzed by using Western blot. *B*) BMMs were treated with VX-745 or RANKL in the presence of M-CSF for 4 d, then stimulated with MG132 (1 μM) for 48 h. Indicated proteins were analyzed by using Western blot. *C*) BMMs, treated or untreated with VX-745, in the presence of RANKL (12.5 ng/ml) and cycloheximide (CHX) (10 μM) for indicated times were analyzed by using Western blot for the expression of β-catenin. *D, E*) BMMs were

(*continued on next page*)

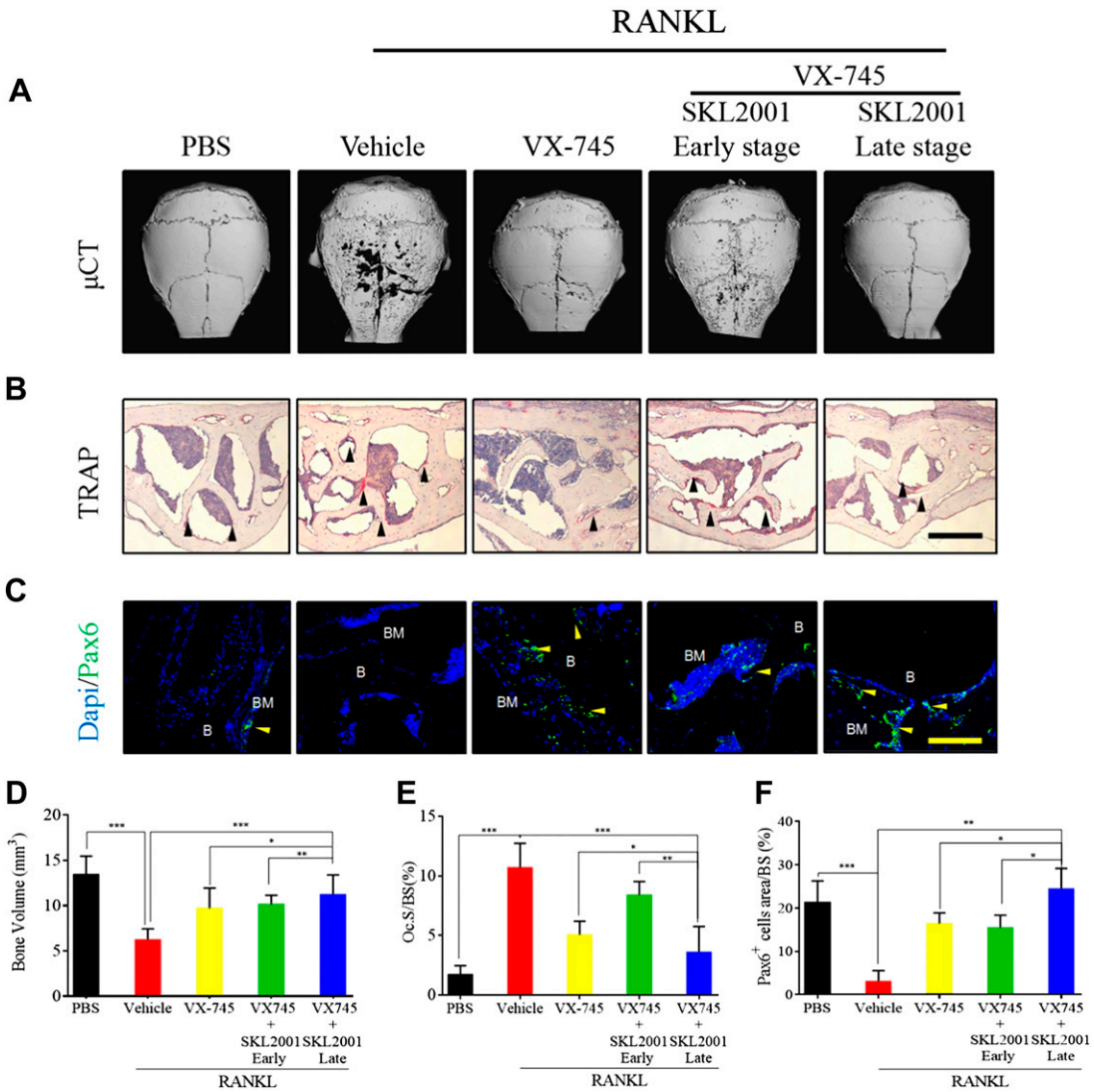

Figure 5. RANKL-induced calvarial bone loss was reversed by VX-745 and SKL2001. *A*) Micro-computed tomography analyses were performed with calvaria from mice that received PBS or RANKL-soaked collagen implants and injection of VX-745 and SKL2001. Representative 3-dimensional reconstructed images. *B*) TRAP staining of calvarial tissue sections. *C*) Calvarial tissue sections stained for Pax6 by immunofluorescence assay. *D*) BV analysis. *E*) Ratio of OC.S/BS (%). *F*) Ratio of Pax6-positive cell area to the total bone surface area. All experiments were performed at ≥3 times; data are presented as means ± SD. Scale bars, 100 μm. One-way ANOVA followed by Tukey's *post hoc* analysis was performed. $*P < 0.05$, $**P < 0.01$, $***P < 0.005$. B, bone; BM, bone marrow.

might be other regulatory pathways involved in the early stage of OC formation. To further investigate the role of p38/β-catenin signaling at a late stage of OC formation, we found that inhibition of p38 reduced the ubiquitin-mediated degradation of β-catenin and that the expression of β-catenin in pre-OCs treated with VX-745 was higher than in the control group. In addition, VX-745 in combination with SKL2001 showed higher efficiency in inhibition of osteoclastogenesis. In line with the *in vitro* assays, RANKL-induced calvarial bone loss was dramatically attenuated by application of VX-745 combined with SKL2001. Thus, in addition to the classic p38/c-Fos/NFATc1 axis, we propose a model for p38-mediated negative regulation of osteoclastogenesis through decreased degradation of β-catenin and up-regulation of Pax6 (**Fig. 6**).

In summary, our study describes a novel regulatory pathway constituting a p38/β-catenin/Pax6 axis at a late stage of osteoclastogenesis. We also propose a novel potential

treated with VX-745 on d 2 during osteoclastogenesis, and the pre-OCs were then transfected with negative control (NC) siRNA or β-catenin siRNA on d 4. TRAP staining assay was performed to calculate the number of OCs (*D*), and Western blot (*E*) was used to analyze the expression of indicated proteins. *F*, *G*) BMMs were treated with VX-745 on d 2 during osteoclastogenesis, and the BMMs were then treated with SKL2001 on d 4 during osteoclastogenesis. TRAP staining assay was performed to calculate the number of OCs (*F*), and Western blotting assay (*G*) was used to analyze the expression of indicated proteins. All experiments were performed ≥3 times; data are presented as means ± SD. Scale bar, 100 μm. One-way ANOVA followed by Tukey's *post hoc* analysis was performed. $*P < 0.05$, $**P < 0.01$, $***P < 0.005$.

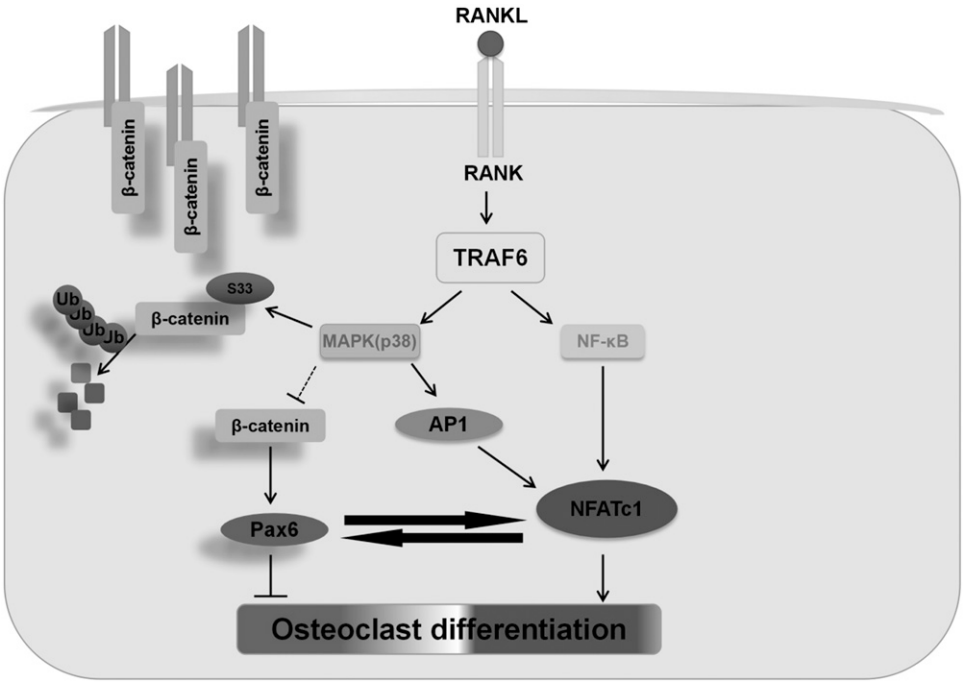

Figure 6. Schematic model for the role of p38/β-catenin/Pax6 in osteoclastogenesis.

therapeutic strategy against OC-related diseases through the use of small molecular inhibitors such as VX-745 and SKL2001. FJ

ACKNOWLEDGMENTS

The authors thank Dr. Xiangqian Fang (Sir Run Run Shaw Hospital) for contributing to revisions to the manuscript. This research was supported by the National Key Research and Development Program of China (2018YFC1105200 to S.F.), the Key Research and Development Plan in Zhejiang Province (2018C03060), the National Nature Science Fund of China [81871797, 81802680 (to S.F.), and 81772387], and the Natural Science Fund of Zhejiang Province (Z15H060002). The authors declare no conflicts of interest.

AUTHOR CONTRIBUTIONS

Z. Jie and Z. Xie conceived and designed the experiments; Z. Jie, S. Shen, X. Zhao, X. Zhang, P. Tang, and Z. Xie performed the *in vitro* experiments; Z. Jie, X. Zhao, W. Xu, and B. Huang conducted the *in vivo* experiments; Z. Jie, A. Qin, S. Fan, and Z. Xie analyzed the data; S. Shen, A. Qin, S. Fan, and Z. Xie supervised the experiments; Z. Jie and Z. Xie drafted the manuscript; A. Qin, S. Fan, and Z. Xie revised the manuscript; and all authors approved the final version of the manuscript.

REFERENCES

1. Grabowski, P. (2009) Physiology of bone. *Endocr. Dev.* **16**, 32–48
2. Lagasse, E., and Weissman, I. L. (1997) Enforced expression of Bcl-2 in monocytes rescues macrophages and partially reverses osteopetrosis in op/op mice. *Cell* **89**, 1021–1031
3. Ninomiya-Tsuji, J., Kishimoto, K., Hiyama, A., Inoue, J., Cao, Z., and Matsumoto, K. (1999) The kinase TAK1 can activate the NIK-I kappaB as well as the MAP kinase cascade in the IL-1 signalling pathway. *Nature* **398**, 252–256
4. Gingery, A., Bradley, E., Shaw, A., and Oursler, M. J. (2003) Phosphatidylinositol 3-kinase coordinately activates the MEK/ERK and AKT/NFkappaB pathways to maintain osteoclast survival. *J. Cell. Biochem.* **89**, 165–179
5. Li, C., Yang, Z., Li, Z., Ma, Y., Zhang, L., Zheng, C., Qiu, W., Wu, X., Wang, X., Li, H., Tang, J., Qian, M., Li, D., Wang, P., Luo, J., and Liu, M. (2011) Maslinic acid suppresses osteoclastogenesis and prevents ovariectomy-induced bone loss by regulating RANKL-mediated NF-κB and MAPK signaling pathways. *J. Bone Miner. Res.* **26**, 644–656
6. Yasui, T., Kadono, Y., Nakamura, M., Oshima, Y., Matsumoto, T., Masuda, H., Hirose, J., Omata, Y., Yasuda, H., Imamura, T., Nakamura, K., and Tanaka, S. (2011) Regulation of RANKL-induced osteoclastogenesis by TGF-β through molecular interaction between Smad3 and Traf6. *J. Bone Miner. Res.* **26**, 1447–1456
7. Monje, P., Hernández-Losa, J., Lyons, R. J., Castellone, M. D., and Gutkind, J. S. (2005) Regulation of the transcriptional activity of c-Fos by ERK. A novel role for the prolyl isomerase PIN1. *J. Biol. Chem.* **280**, 35081–35084
8. Yu, B., Chang, J., Liu, Y., Li, J., Kevork, K., Al-Hezaimi, K., Graves, D. T., Park, N. H., and Wang, C. Y. (2014) Wnt4 signaling prevents skeletal aging and inflammation by inhibiting nuclear factor-κB. *Nat. Med.* **20**, 1009–1017; erratum: 21, 1101
9. Sharma, S. M., Bronisz, A., Hu, R., Patel, K., Mansky, K. C., Sif, S., and Ostrowski, M. C. (2007) MITF and PU.1 recruit p38 MAPK and NFATc1 to target genes during osteoclast differentiation. *J. Biol. Chem.* **282**, 15921–15929
10. Rodríguez-Carballo, E., Gámez, B., and Ventura, F. (2016) p38 MAPK signaling in osteoblast differentiation. *Front. Cell Dev. Biol.* **4**, 40
11. Deepak, V., Kruger, M. C., Joubert, A., and Coetzee, M. (2015) Piperine alleviates osteoclast formation through the p38/c-Fos/NFATc1 signaling axis. *Biofactors* **41**, 403–413
12. Bopp, D., Burri, M., Baumgartner, S., Frigerio, G., and Noll, M. (1986) Conservation of a large protein domain in the segmentation gene paired and in functionally related genes of Drosophila. *Cell* **47**, 1033–1040
13. Dahl, E., Koseki, H., and Balling, R. (1997) Pax genes and organogenesis. *BioEssays* **19**, 755–765
14. Delogu, A., Schebesta, A., Sun, Q., Aschenbrenner, K., Perlot, T., and Busslinger, M. (2006) Gene repression by Pax5 in B cells is essential for blood cell homeostasis and is reversed in plasma cells. *Immunity* **24**, 269–281
15. Hinoi, E., Nakatani, E., Yamamoto, T., Iezaki, T., Takahata, Y., Fujita, H., Ishiura, R., Takamori, M., and Yoneda, Y. (2012) The transcription factor paired box-5 promotes osteoblastogenesis through direct induction of osterix and osteocalcin. *J. Bone Miner. Res.* **27**, 2526–2534
16. Kogawa, M., Hisatake, K., Atkins, G. J., Findlay, D. M., Enoki, Y., Sato, T., Gray, P. C., Kanesaki-Yatsuka, Y., Anderson, P. H., Wada, S., Kato,

N., Fukuda, A., Katayama, S., Tsujimoto, M., Yoda, T., Suda, T., Okazaki, Y., and Matsumoto, M. (2013) The paired-box homeodomain transcription factor Pax6 binds to the upstream region of the TRAP gene promoter and suppresses receptor activator of NF-κB ligand (RANKL)-induced osteoclast differentiation. *J. Biol. Chem.* **288**, 31299–31312
17. Takayanagi, H., Ogasawara, K., Hida, S., Chiba, T., Murata, S., Sato, K., Takaoka, A., Yokochi, T., Oda, H., Tanaka, K., Nakamura, K., and Taniguchi, T. (2000) T-cell-mediated regulation of osteoclastogenesis by signalling cross-talk between RANKL and IFN-gamma. *Nature* **408**, 600–605
18. Mikkola, I., Bruun, J. A., Bjorkoy, G., Holm, T., and Johansen, T. (1999) Phosphorylation of the transactivation domain of Pax6 by extracellular signal-regulated kinase and p38 mitogen-activated protein kinase. *J. Biol. Chem.* **274**, 15115–15126
19. Hadjal, Y., Hadadeh, O., Yazidi, C. E., Barruet, E., and Binétruy, B. (2013) A p38MAPK-p53 cascade regulates mesodermal differentiation and neurogenesis of embryonic stem cells. *Cell Death Dis.* **4**, e737
20. McGuire, V. A., Gray, A., Monk, C. E., Santos, S. G., Lee, K., Aubareda, A., Crowe, J., Ronkina, N., Schwermann, J., Batty, I. H., Leslie, N. R., Dean, J. L., O'Keefe, S. J., Boothby, M., Gaestel, M., and Arthur, J. S. (2013) Cross talk between the Akt and p38α pathways in macrophages downstream of toll-like receptor signaling. *Mol. Cell. Biol.* **33**, 4152–4165
21. Xie, Z., Yu, H., Sun, X., Tang, P., Jie, Z., Chen, S., Wang, J., Qin, A., and Fan, S. (2018) A novel diterpenoid suppresses osteoclastogenesis and promotes osteogenesis by inhibiting ifrd1-mediated and IκBα-mediated p65 nuclear translocation. *J. Bone Miner. Res.* **33**, 667–678
22. Kim, H., Lee, Y. D., Kim, H. J., Lee, Z. H., and Kim, H. H. (2017) SOD2 and Sirt3 control osteoclastogenesis by regulating mitochondrial ROS. *J. Bone Miner. Res.* **32**, 397–406
23. Bouxsein, M. L., Boyd, S. K., Christiansen, B. A., Guldberg, R. E., Jepsen, K. J., and Müller, R. (2010) Guidelines for assessment of bone microstructure in rodents using micro-computed tomography. *J. Bone Miner. Res.* **25**, 1468–1486
24. Dempster, D. W., Compston, J. E., Drezner, M. K., Glorieux, F. H., Kanis, J. A., Malluche, H., Meunier, P. J., Ott, S. M., Recker, R. R., and Parfitt, A. M. (2013) Standardized nomenclature, symbols, and units for bone histomorphometry: a 2012 update of the report of the ASBMR Histomorphometry Nomenclature Committee. *J. Bone Miner. Res.* **28**, 2–17
25. Wei, W., Zeve, D., Suh, J. M., Wang, X., Du, Y., Zerwekh, J. E., Dechow, P. C., Graff, J. M., and Wan, Y. (2011) Biphasic and dosage-dependent regulation of osteoclastogenesis by β-catenin. *Mol. Cell. Biol.* **31**, 4706–4719
26. Gan, Q., Lee, A., Suzuki, R., Yamagami, T., Stokes, A., Nguyen, B. C., Pleasure, D., Wang, J., Chen, H. W., and Zhou, C. J. (2014) Pax6 mediates ß-catenin signaling for self-renewal and neurogenesis by neocortical radial glial stem cells. *Stem Cells* **32**, 45–58
27. Ash, P., Loutit, J. F., and Townsend, K. M. (1980) Osteoclasts derived from haematopoietic stem cells. *Nature* **283**, 669–670
28. Takayanagi, H., Kim, S., Koga, T., Nishina, H., Isshiki, M., Yoshida, H., Saiura, A., Isobe, M., Yokochi, T., Inoue, J., Wagner, E. F., Mak, T. W., Kodama, T., and Taniguchi, T. (2002) Induction and activation of the transcription factor NFATc1 (NFAT2) integrate RANKL signaling in terminal differentiation of osteoclasts. *Dev. Cell* **3**, 889–901
29. Manolagas, S. C., and Jilka, R. L. (1995) Bone marrow, cytokines, and bone remodeling. Emerging insights into the pathophysiology of osteoporosis. *N. Engl. J. Med.* **332**, 305–311
30. Takayanagi, H. (2007) Osteoimmunology: shared mechanisms and crosstalk between the immune and bone systems. *Nat. Rev. Immunol.* **7**, 292–304
31. Enslen, H., Brancho, D. M., and Davis, R. J. (2000) Molecular determinants that mediate selective activation of p38 MAP kinase isoforms. *EMBO J.* **19**, 1301–1311
32. Roodman, G. D. (2004) Mechanisms of bone metastasis. *N. Engl. J. Med.* **350**, 1655–1664
33. Greenblatt, M. B., Shim, J. H., Zou, W., Sitara, D., Schweitzer, M., Hu, D., Lotinun, S., Sano, Y., Baron, R., Park, J. M., Arthur, S., Xie, M., Schneider, M. D., Zhai, B., Gygi, S., Davis, R., and Glimcher, L. H. (2010) The p38 MAPK pathway is essential for skeletogenesis and bone homeostasis in mice. *J. Clin. Invest.* **120**, 2457–2473
34. Cong, Q., Jia, H., Li, P., Qiu, S., Yeh, J., Wang, Y., Zhang, Z. L., Ao, J., Li, B., and Liu, H. (2017) p38α MAPK regulates proliferation and differentiation of osteoclast progenitors and bone remodeling in an aging-dependent manner. *Sci. Rep.* **7**, 45964
35. Böhm, C., Hayer, S., Kilian, A., Zaiss, M. M., Finger, S., Hess, A., Engelke, K., Kollias, G., Krönke, G., Zwerina, J., Schett, G., and David, J. P. (2009) The alpha-isoform of p38 MAPK specifically regulates arthritic bone loss. *J. Immunol.* **183**, 5938–5947
36. Yamashita, T., Kobayashi, Y., Mizoguchi, T., Yamaki, M., Miura, T., Tanaka, S., Udagawa, N., and Takahashi, N. (2008) MKK6-p38 MAPK signaling pathway enhances survival but not bone-resorbing activity of osteoclasts. *Biochem. Biophys. Res. Commun.* **365**, 252–257
37. Chi, N., and Epstein, J. A. (2002) Getting your Pax straight: Pax proteins in development and disease. *Trends Genet.* **18**, 41–47
38. Huang, H., Ryu, J., Ha, J., Chang, E. J., Kim, H. J., Kim, H. M., Kitamura, T., Lee, Z. H., and Kim, H. H. (2006) Osteoclast differentiation requires TAK1 and MKK6 for NFATc1 induction and NF-kappaB transactivation by RANKL. *Cell Death Differ.* **13**, 1879–1891
39. Lin, J., Lee, D., Choi, Y., and Lee, S. Y. (2015) The scaffold protein RACK1 mediates the RANKL-dependent activation of p38 MAPK in osteoclast precursors. *Sci. Signal.* **8**, ra54
40. Glass D. A. II, Bialek, P., Ahn, J. D., Starbuck, M., Patel, M. S., Clevers, H., Taketo, M. M., Long, F., McMahon, A. P., Lang, R. A., and Karsenty, G. (2005) Canonical Wnt signaling in differentiated osteoblasts controls osteoclast differentiation. *Dev. Cell* **8**, 751–764
41. Suzuki, A., Guicheux, J., Palmer, G., Miura, Y., Oiso, Y., Bonjour, J. P., and Caverzasio, J. (2002) Evidence for a role of p38 MAP kinase in expression of alkaline phosphatase during osteoblastic cell differentiation. *Bone* **30**, 91–98
42. Zhou, F. H., Foster, B. K., Zhou, X. F., Cowin, A. J., and Xian, C. J. (2006) TNF-alpha mediates p38 MAP kinase activation and negatively regulates bone formation at the injured growth plate in rats. *J. Bone Miner. Res.* **21**, 1075–1088
43. Rey, A., Manen, D., Rizzoli, R., Ferrari, S. L., and Caverzasio, J. (2007) Evidences for a role of p38 MAP kinase in the stimulation of alkaline phosphatase and matrix mineralization induced by parathyroid hormone in osteoblastic cells. *Bone* **41**, 59–67
44. Cott, C., Thuenauer, R., Landi, A., Kühn, K., Juillot, S., Imberty, A., Madl, J., Eierhoff, T., and Römer, W. (2016) Pseudomonas aeruginosa lectin LecB inhibits tissue repair processes by triggering β-catenin degradation. *Biochim. Biophys. Acta* **1863** (6 Pt A), 1106–1118
45. Xu, W., and Kimelman, D. (2007) Mechanistic insights from structural studies of beta-catenin and its binding partners. *J. Cell Sci.* **120**, 3337–3344

Received for publication September 15, 2018.
Accepted for publication November 12, 2018.